

**NASA CONTRACTOR  
REPORT**

NASA CR-1832



NASA CR-1832

C.1

0061113



LOAN COPY: RETURN TO  
AFWL (DOGL)  
KIRTLAND AFB, N. M.

**THE CALCULATION OF OPTIMAL  
LININGS FOR JET ENGINE  
INLET DUCTS - PART II**

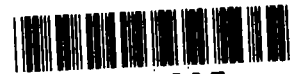
*by J. P. D. Wilkinson*

*Prepared by*

GENERAL ELECTRIC RESEARCH AND DEVELOPMENT CENTER  
Schenectady, N.Y.

*for*

NATIONAL AERONAUTICS AND SPACE ADMINISTRATION • WASHINGTON, D. C. • AUGUST 1971



0061113

1. Report No. NASA CR-1832	2. Government Accession No.	3. Recipient's Catalog No.	
4. Title and Subtitle THE CALCULATION OF OPTIMAL LININGS FOR JET ENGINE INLET DUCTS - PART II		5. Report Date August, 1971	6. Performing Organization Code
		8. Performing Organization Report No.	
7. Author(s) J. P. D. Wilkinson		10. Work Unit No.	
9. Performing Organization Name and Address General Electric Research and Development Center Schenectady, New York		11. Contract or Grant No. NASW 1922	
		13. Type of Report and Period Covered Contractor Report	
12. Sponsoring Agency Name and Address National Aeronautics and Space Administration Washington, D. C., 20546		14. Sponsoring Agency Code	
15. Supplementary Notes Part I "The Theoretical and Experimental Investigations on Multiple Pure Tone Noise" by R. A. Kantola and M. Kurosaka - NASA CR-1831			
16. Abstract <p>A numerical method is presented for calculating the optimal lining impedance for the inlet duct of a jet engine. The calculation is based on the condition that the total radiated power from the duct shall be a minimum. Several situations are considered: first, the case of an axially symmetric duct in a stationary acoustic medium; second, that of a body of arbitrary geometry in a stationary medium; and finally, the case of an axially symmetric duct in the presence of spinning modes and axial air flow. In each case, the method may yield the optimal lining impedances for a given discrete frequency, flow velocity, and duct geometry.</p> <p>To demonstrate the application of the method, a number of cases are investigated. First, a cylindrical duct closed at one end with a vibrating piston is used to make comparisons with predictions obtained analytically by Rice. Then a more complex problem of a bell-mouth compressor is investigated. A discussion of the results obtained is presented, together with a critique of the potential difficulties of the method as applied to complex duct configurations.</p>			
17. Key Words (Suggested by Author(s)) Noise Acoustic Lining Duct Lining		18. Distribution Statement Unclassified - Unlimited	
19. Security Classif. (of this report) Unclassified	20. Security Classif. (of this page) Unclassified	21. No. of Pages 32	22. Price* \$3.00



## FOREWORD

This report was prepared under Contract No. NASW-1922 for NASA Headquarters, Office of Advanced Research and Technology, Research Division, under the technical direction of Mr. I. R. Schwartz. The work was conducted at the Mechanical Engineering Laboratory, General Electric Research and Development Center in Schenectady, New York.



## Table of Contents

<u>Section</u>	<u>Title</u>	<u>Page</u>
	List of Illustrations	vi
	List of Symbols	vii
I	Introduction	1
II	Mathematical Formulation	2
III	Stationary Medium	4
	a) Axially Symmetric Geometry	4
	b) Arbitrary Geometry	6
IV	Moving Medium in the Presence of Spinning Modes - Axially Symmetric Geometry	9
V	Numerical Results	12
	a) Cylindrical Duct	12
	b) Bell-Mouth Duct	13
VI	Conclusions	15
VII	References	16

## List of Illustrations

<u>Figure</u>	<u>Title</u>	
1	Schematic of a Jet Engine	19
2	The Closed Surface $S_1 + S_2$	20
3	Axially Symmetric Body in a Stationary Medium	21
4	Cylindrical Duct Geometry	22
5	Optimization Paths in the Impedance Plane	23
6	Distribution of Absorbed Energy	24
7	Geometry of Bell-Mouth Duct	25
8	Far Field Pressures at 15 Feet from the Duct Mouth	26

## List of Tables

1	Energy Absorption in a Cylindrical Duct	17
II	Summary of Energy Calculations	
	Normalized Velocity	18
	Normalized Source Energy	18

## List of Symbols

A	source strength coefficient
c	speed of sound in fluid
E	radiated power
g	number of circumferential lobes
M	Mach number $V/c$
p	pressure
$p_0$	prescribed pressure on a boundary
R	radial distance
r	radius
S	surface area
t	time
u	velocity
$u_0$	prescribed velocity on a boundary
V	flow velocity
x	axial coordinate
Z	impedance
N, i, j, k, n, M	integers
$\partial/\partial n, \partial/\partial N$	denotes differentiation with respect to a normal
$\eta, \mu$	orthogonal surface coordinates
$\eta_0, \mu_0$	perimeter along $\eta$ and $\mu$
v	equal to $\omega/c$
$\rho$	fluid density
$\sigma$	source strength distribution
$\Phi, \phi$	velocity potential
$\omega$	frequency
$\nabla^2$	Laplacian operator
$\wedge$	denotes a complex quantity
*	denotes a complex conjugate
R	subscript denotes the real part
I	subscript denotes the imaginary part



## I. INTRODUCTION

Noise is radiated from a number of sources in a jet engine. One source of particular importance is due to the air flow through the compressor blades of the jet engine. The spectrum of the noise from the source consists of a number of discrete frequency bands at the blade passing frequencies. As described by Tyler and Sofrin (Ref. 1), the effect of the interaction of the stator and rotor blades in the compressor is to produce a rotating source of sound at these blade passing frequencies. The radiation of these so-called spinning modes down the inlet duct through which air flows is a complicated phenomenon, particularly since the duct geometry is not uniform.

Various methods have been used to reduce the noise level due to the compressor blades. One technique has been to coat the inside of the duct walls with a material of a certain acoustic impedance, so that the noise is attenuated as it propagates down the duct (see Figure 1). In the past, the acoustic impedance of this lining has been determined in an empirical manner, or else by means of rather simplified analyses (see, for example, Refs. 2 and 3), which may not adequately reflect the geometry of the situation.

Intuitively, one would suspect that there exists a lining impedance which absorbs more energy from the sound source than any other lining could. Such a lining would then be an optimal lining. The total sound power radiated from the duct would have a minimum possible value. The impedance distribution of this lining can be calculated in precisely this manner: we require that the impedance of the lined portion of the duct be adjusted such that the radiated energy be minimized. A method whereby this minimization may be achieved will be described in this report.

A new analytical technique which offers much promise for the study of sound radiation in ducts of arbitrary shape in the presence of spinning modes and axial air flow has been described by Martenson and Liu (Ref. 4). They have developed a numerical method whereby such radiation may be predicted, given the characteristics of the source of sound (e.g., the pressure field at the compressor blades), the Mach number of the flow, the shape of the inside and outside of the duct, and the rigidity or acoustic impedance of the duct walls. A modification of this method, to be described in this report, will allow the calculation of the lining impedance which yields the minimum total radiated power.

## II. MATHEMATICAL FORMULATION

The propagation of an acoustic disturbance in a fluid medium is governed by a velocity potential

$$\hat{\phi} = \hat{\phi} e^{i\omega t} \quad (2.1)$$

which satisfies the reduced wave equation

$$\nabla^2 \hat{\phi} + v^2 \hat{\phi} = 0 \quad (2.2)$$

where

$$v = \omega/c \quad (2.3)$$

and  $c$  is the speed of sound in the fluid. The pressure  $\hat{p}$  and particle velocity  $\hat{u}$  in the fluid are related to the velocity potential  $\hat{\phi}$  by the expressions

$$\hat{p} = i\omega\rho\hat{\phi} \quad (2.4)$$

$$\hat{u} = \partial\hat{\phi}/\partial n \quad (2.5)$$

When sound is radiated from a closed body whose surface is denoted by  $S_1+S_2$  (see Figure 2), a solution to Equation (2.2) can be written in the form

$$\hat{\phi}(p) = \iint_{S_1+S_2} \hat{\sigma}(S) \frac{e^{ivR}}{R} dS \quad (2.6)$$

Here  $\hat{\sigma}(S)$  represents a source sheet overlaying the surface  $S_1+S_2$ , whose strength must be adjusted to satisfy the following boundary conditions:

$$\left. \begin{array}{l} \text{either } \hat{p} = \hat{p}_0 \\ \text{or } \hat{u} = \hat{u}_0 \end{array} \right\} \text{ on } S_1 \quad (2.7)$$

and on  $S_2$  the impedance  $\hat{Z}$  is to be given in a manner to be explained soon.

In the process of lining optimization, we require that the absorbed power  $E_a$  on  $S_2$  be maximized, where

$$E_a = -\frac{1}{2} \iint_{S_2} (\hat{p}^* \hat{u} + \hat{u}^* \hat{p}) dS \quad (2.8)$$

To maximize  $E_a$ , we start with an initial feasible solution, which merely represents a situation with a physically realistic lining

on  $S_2$ . For example, one might begin by calculating  $E_a$  for the case where the lining had a characteristic impedance,  $Z = \rho c$ . This lining would not in general be optimal, but it would be a reasonable initial feasible solution. The process of maximization is continued by perturbing the value of  $Z$  about the initial solution, and calculating where the gradient  $\partial E_a / \partial Z$  is the steepest. A step in  $Z$  is made in this direction, and the process is again repeated until a local maximum in  $E_a$  is achieved.

One should note that one could equally well minimize the radiated power in the far field,  $E_f$ . The process is identical, and in fact,  $E_f$  should be minimized automatically when  $E_a$  is maximized. However, for convenience in numerical computation, one or the other can be chosen.

Whereas the process of maximization is very simple in principle, it is nevertheless rather complicated to put into practice. First, at each perturbation of  $Z$  one must make calculations of  $E_a$ , which require extensive numerical computations. Second, the numerical gradient techniques can be rather complicated. Fortunately, we have available the acoustic computer codes of Liu and Martenson (Ref. 4) for the rapid calculation of  $E_a$  for bodies of arbitrary shape. In addition, various automatic gradient techniques have been programmed: we are using a computer code known as ADOPT (Automatic Design Optimization, see Ref. 5). The advantage of this numerical method is that it promises to be entirely automatic once an initial feasible solution is selected.

In the following sections, a method will be given for determining the optimal impedance  $Z(S_2)$ . Several situations will be considered, namely, the case of a stationary medium with either an axially symmetric geometry or with an arbitrary three-dimensional geometry, and the case of a moving medium with an axially symmetric geometry and in the presence of spinning modes typical of a jet engine inlet duct.

### III. STATIONARY MEDIUM

#### a) Axially Symmetric Geometry

Consider an axially symmetric closed surface  $S_1+S_2$  (see Figure 3). Let this surface be divided into two portions. On the surface  $S_1$  we specify certain boundary conditions, whereas an optimal lining must be calculated on surface  $S_2$ . Let surface  $S_1$  be divided into  $K$  rings and  $S_2$  be divided into  $M$  rings, each ring being of surface area  $\Delta S_j$  ( $j = 1, \dots, K, K+1, \dots, M$ ) and radius  $r_j$ .

The source strength  $\hat{\sigma}(S)$  is now expressed as a truncated Fourier series of  $2N$  terms

$$\hat{\sigma}(S) = \sum_{n=1}^N \left[ \hat{A}_{(2n-1)} \cos \frac{2\pi(n-1)\eta}{\eta_0} + \hat{A}_{2n} \sin \frac{2\pi n\eta}{\eta_0} \right] \quad (3.1)$$

Here  $\eta_0$  is the total perimeter of the surface  $S_1+S_2$  in a plane containing the axis of revolution.

At a point on the  $j$ -th ring, the pressure  $\hat{p}_j$  is given by

$$\hat{p}_j = i\omega\rho \iint_{S_1+S_2} \hat{\sigma}(S) \frac{e^{i\nu R}}{R} dS \quad (3.2)$$

By assuming that the source strength is constant over each ring, we may write

$$\hat{p}_j = i\omega\rho \sum_{i=1}^{K+M} \hat{\sigma}(S_i) \iint_{\Delta S_i} \frac{e^{i\nu R_{ij}}}{R_{ij}} dS_i \quad (3.3)$$

where  $R_{ij}$  is the distance from the receiving ring  $j$  to the source ring  $i$ , and is given by

$$R_{ij}^2 = (x_i - x_j)^2 + r_j^2 - 2r_i r_j \cos\theta \quad (3.4)$$

By using Equation (3.1), we may now express the pressure as

$$\hat{p}_j = \sum_{n=1}^{2N} \hat{A}_n \hat{\alpha}_{nj} \quad (3.5)$$

where

$$\hat{\alpha}_{nj} = \begin{cases} i\omega\rho \sum_{i=1}^{K+M} \cos \frac{\pi(n-1)\eta_i}{\eta_o} \iint_{\Delta S_i} \frac{e^{i\nu R_{ij}}}{R_{ij}} dS_i & (n \text{ odd}) \\ i\omega\rho \sum_{i=1}^{K+M} \sin \frac{\pi n \eta_i}{\eta_o} \iint_{\Delta S_i} \frac{e^{i\nu R_{ij}}}{R_{ij}} dS_i & (n \text{ even}) \end{cases} \quad (3.6)*$$

Similarly, by virtue of Equations (2.5), (2.6) and (3.1), we write the velocity at the j-th ring as

$$\hat{u}_j = \sum_{n=1}^{2N} \hat{A}_n \hat{\beta}_{nj} \quad (3.7)$$

where

$$\hat{\beta}_{nj} = \begin{cases} \sum_{i=1}^{K+M} \cos \frac{\pi(n-1)\eta_i}{\eta_o} \iint_{\Delta S_i} \frac{\partial}{\partial N_i} \frac{e^{i\nu R_{ij}}}{R_{ij}} dS_i & (n \text{ odd}) \\ \sum_{i=1}^{K+M} \sin \frac{\pi n \eta_i}{\eta_o} \iint_{\Delta S_i} \frac{\partial}{\partial N_i} \frac{e^{i\nu R_{ij}}}{R_{ij}} dS_i & (n \text{ even}) \end{cases} \quad (3.8)*$$

On the surface  $S_1$  the boundary conditions of Equation (2.8) must be satisfied. Because the surface is divided into K rings, we require that the K separate conditions

$$\left. \begin{aligned} \hat{u}_i &= \hat{u}_{oi} \\ \hat{p}_i &= \hat{p}_{oi} \end{aligned} \right\} (i=1, \dots, K) \quad (3.9)$$

be satisfied. On the lining surface  $S_2$  we require that

$$\hat{z} = \hat{z}_{oi} \quad (i=1, \dots, M) \quad (3.10)$$

where  $Z_{oi}$  is the impedance at the point i at that particular stage in the optimization.

Substitution of the series (3.5) and (3.7) into the conditions (3.9) and (3.10) yields a set of K+M linear algebraic equations in

\* It should be noted that the integrals appearing in Equations (3.6) and (3.8) are singular when  $i=j$ . However, the singularities are integrable and integrals may be evaluated as improper integral, the principal values in each case being 0 and  $-2\pi$ , respectively.

2N unknowns. Usually  $2N \leq K+M$ , so that the equations may be overdetermined. They may be solved by a least squares method such that the square of the error at each point is minimized. Once the source strengths  $A_n$  are found, it is a simple matter to compute all other required quantities from the given equations.

The power  $E_j$  radiated by the  $j$ -th ring may be written as follows:

$$E_j = \frac{1}{2}(p_j u_j^* + p_j^* u_j) \Delta S_j \quad (3.11)$$

The power absorbed by the lining is given by

$$E_a = \sum_{j=1}^M E_j \quad (3.12)$$

The total power radiated from the active sources (e.g., pistons or blades) on the surface  $S_1$  is given by

$$E_s = \sum_{j=1}^K E_j \quad (3.13)$$

The energy that reaches the far field can also be calculated by computing  $p$  and  $u$  there, and carrying out the sum indicated in (3.11).

By perturbing the impedances  $Z_{oi}$  and calculating the path of steepest ascent of  $E_a$ , we can now climb automatically toward the lining impedance that yields a maximum of  $E_a$ .

#### b) Arbitrary Geometry

A body whose surface  $S_1+S_2$  is of arbitrary shape can be considered in a similar manner. We express the source strength as a truncated Fourier series in two variables  $\eta$  and  $\mu$  so that at the point  $j$  its strength is

$$\hat{\sigma}_j = \sum_{n=1}^N \hat{A}_n \hat{a}_{jn}(\eta_j, \mu_j) \quad (3.14)$$

For example, a double Fourier series can be written as

$$\hat{\sigma}(\eta, \mu) = \sum_{j=0}^{J-1} \sum_{\ell=0}^{L-1} \hat{a}_{j\ell} \cos \frac{2\pi j\eta}{\eta_0} \cos \frac{2\pi \ell\mu}{\mu_0}$$

$$\begin{aligned}
& + \sum_{j=0}^{J-1} \sum_{\ell=1}^L \hat{b}_{j\ell} \cos \frac{2\pi j\eta}{\eta_0} \cos \frac{2\pi\ell\mu}{\eta_0} \\
& + \sum_{j=1}^J \sum_{\ell=0}^{L-1} \hat{c}_{j\ell} \sin \frac{2\pi j\eta}{\eta_0} \cos \frac{2\pi\ell\mu}{\eta_0} \\
& + \sum_{j=1}^J \sum_{\ell=1}^L \hat{d}_{j\ell} \sin \frac{2\pi j\eta}{\eta_0} \sin \frac{2\pi\ell\mu}{\eta_0}
\end{aligned} \tag{3.15}$$

and a simple transformation yields the series in the form of Equation (3.14).

We now break the surface into a number of quadrilateral elements of area  $\Delta S_j$  upon which the source strength is assumed constant. Then the pressure at a point  $j$  can be expressed in series form by means of Equation (3.2) (which is also valid in a three-dimensional geometry) as follows:

$$\hat{p}_j = \sum_{n=1}^N \hat{A}_n \hat{\alpha}_{nj} \tag{3.16}$$

where

$$\hat{\alpha}_{nj} = i\omega\rho \sum_{i=1}^{K+M} \hat{a}_{jn} \iint_{\Delta S_j} \frac{e^{i\nu R_{ij}}}{R_{ij}} dS_i \tag{3.17}$$

Similarly, the fluid velocity may be written as

$$\hat{u}_j = \sum_{n=1}^N \hat{A}_n \hat{\beta}_{nj} \tag{3.18}$$

where

$$\hat{\beta}_{nj} = \sum_{i=1}^{K+M} \hat{a}_{jn} \hat{\psi}_{ij} \tag{3.19}$$

and

$$\hat{\psi}_{ij} = \begin{cases} \iint_{\Delta S_i} \frac{\partial}{\partial N_i} \frac{e^{i\nu R_{ij}}}{R_{ij}} dS_i & i \neq j \\ -2\pi & i = j \end{cases} \tag{3.20}$$

The form of pressure and velocity in this three-dimensional geometry is now identical with that of the axially symmetric geometry given by Equations (3.5) and (3.7). Thus, the remainder of the analysis follows in the same manner. The solution yields the source strength  $\hat{\sigma}$ , from which can be computed the absorbed and radiated powers  $E_a$  and  $E_s$ . They may be used to calculate the optimal impedance by using the gradient method previously described.



IV. MOVING MEDIUM IN THE PRESENCE OF SPINNING MODES -  
AXIALLY SYMMETRIC GEOMETRY

The previous analysis referred to a stationary medium. To model more closely the noise propagation at the inlet duct of a jet engine, it is necessary to consider the presence of spinning modes due to the compressor blades, and the overall flow of the inlet air through the duct. To this end we shall consider the radiation of sound from a body  $S_1+S_2$  in a fluid which flows in the x-direction with a velocity  $V$ . In such a moving medium, the sound propagation is governed by a velocity potential  $\hat{\phi}$ , which satisfies the equation

$$\left[ \nabla^2 - M^2 \frac{\partial^2}{\partial x^2} - \frac{2M}{c} \frac{\partial^2}{\partial x \partial t} - \frac{1}{c^2} \frac{\partial^2}{\partial t^2} \right] \hat{\phi} = 0 \quad (4.1)$$

where  $M = V/c$  is the Mach number. The pressure in the fluid is given by

$$\hat{p} = \rho (\partial \hat{\phi} / \partial t + V \partial \hat{\phi} / \partial x) \quad (4.2)$$

and the particle velocity is

$$\hat{u} = \partial \hat{\phi} / \partial x \quad (4.3)$$

When spinning modes are present with  $g$  lobes, we assume that

$$\hat{\phi} = \hat{\phi}_e e^{i(g\theta + \omega t)} \quad (4.4)$$

$$\hat{p} = \hat{p}_e e^{i(g\theta + \omega t)} \quad (4.5)$$

$$\hat{u} = \hat{u}_e e^{i(g\theta + \omega t)} \quad (4.6)$$

A solution to Equation (4.1) is given by

$$\hat{\phi} = \iint_{S_1+S_2} \hat{\sigma}(S) \frac{e^{i\nu R}}{R} dS \quad (4.7)$$

where

$$R^2 = \frac{-M(x-\bar{x}) + [(x-\bar{x})^2 + (1-M^2)(r^2 - \bar{r}^2 - 2\bar{r}r \cos\theta)]}{1-M^2} \quad (4.8)$$

$$(\bar{R})^2 = \frac{(x-\bar{x})^2}{1-M^2} + \bar{r}^2 + r^2 - 2\bar{r}r \cos\theta \quad (4.9)$$

The point  $(\bar{x}, \bar{r})$  is the receiving point and  $(x, r)$  is the source point. The source strength  $\hat{\sigma}(S)$  must be adjusted so that the boundary conditions on the surface  $S_1$  are satisfied, namely,

$$\left. \begin{array}{l} \text{either } \hat{u} = \hat{u}_o \\ \text{or } \hat{p} = \hat{p}_o \end{array} \right\} \text{ on } S_1 \quad (4.10)$$

$$\hat{z} = \hat{z}_{oi} \quad \text{on } S_2 \quad (4.11)$$

where  $Z_{oi}$  is the impedance at the point  $i$  during that particular phase in the optimization process.

As before, we assume that the source strength can be represented by a truncated Fourier series

$$\hat{\sigma}(S) = e^{ig\theta} \sum_{n=1}^N \left\{ \hat{A}_{(2n-1)} \cos \frac{2\pi(n-1)\eta}{\eta_o} + \hat{A}_{2n} \sin \frac{2\pi n\eta}{\eta_o} \right\} \quad (4.12)$$

where  $\eta_o$  is the perimeter of  $S_1+S_2$  in a plane containing the axis of revolution  $x$ . Then, by representing the surfaces  $S_1$  and  $S_2$  as a number of rings of area  $\Delta S_j$  as before, we can write the pressure and the velocity at the  $j$ -th ring in a series form as follows:

$$\hat{p}_j = \sum_{n=1}^{2N} \hat{A}_n \hat{\alpha}_{nj} \quad (4.13)$$

$$\hat{u}_j = \sum_{n=1}^{2N} \hat{A}_n \hat{\beta}_{nj} \quad (4.14)$$

where

$$\hat{\alpha}_{nj} = \begin{cases} \rho \sum_{i=1}^{K+M} \cos\left(\frac{\pi(n-1)\eta_i}{\eta_o}\right) \iint_{\Delta S_i} e^{ig\theta} (i\omega + V \frac{\partial}{\partial x}) \frac{e^{i\nu R_{ij}}}{R_{ij}} dS_i & (n \text{ odd}) \\ \rho \sum_{i=1}^{K+M} \sin\left(\frac{\pi n \eta_i}{\eta_o}\right) \iint_{\Delta S_i} e^{ig\theta} (i\omega + V \frac{\partial}{\partial x}) \frac{e^{i\nu R_{ij}}}{R_{ij}} dS_i & (n \text{ even}) \end{cases} \quad (4.15) *$$

\* The integrals appearing in Equations (4.15) and (4.16) are singular when  $i=j$ . Their principal values are  $-2\pi V/(1-M^2)^{1/2}$  and  $-2\pi(1-M^2)^{1/2}/(1-M^2 D_j)$ , respectively, where  $D_j$  is the direction cosine of the surface normal at the point  $j$  with respect to the  $x$ -axis.

$$\hat{\beta}_{nj} = \begin{cases} \left( \sum_{i=1}^{K+M} \cos\left(\frac{\pi(n-1)\eta_i}{\eta_0}\right) \right) \iint_{\Delta S_i} e^{ig\theta} \frac{\partial}{\partial N_i} \frac{e^{i\nu R_{ij}}}{R_{ij}} dS_i & \text{(n odd)} \\ \left( \sum_{i=1}^{K+M} \sin\left(\frac{\pi n \eta_i}{\eta_0}\right) \right) \iint_{\Delta S_i} e^{ig\theta} \frac{\partial}{\partial N_i} \frac{e^{i\nu R_{ij}}}{R_{ij}} dS_i & \text{(n even)} \end{cases} \quad (4.16)^*$$

Because the pressure and velocity of Equations (4.13) and (4.14) are of a form identical with those of the stationary medium given by Equations (3.5) and (3.7), the remainder of the analysis follows in exactly the same manner as before. The solution for  $A_n$  yields the source strength distribution from which we can find the absorbed power  $E_a$  as before. The optimization process using the gradient technique follows as we described previously.

## V. NUMERICAL RESULTS

### a) Cylindrical Duct

In order to make a comparison of the method described here with existing results, we will study the case of a lined cylindrical duct closed at one end by a vibrating piston that generates a "plane" wave in the duct. Rice (Ref. 2) has studied the attenuation of plane waves down a cylindrical duct, and gives a chart with which we can compare our numerical results.

The duct geometry is shown in Figure 4. The ratio of length to diameter,  $L/D$ , is 1.64. The piston moves at 700 Hz, giving a wavelength  $\lambda = 18.8$  inches in air. The ratio  $D/\lambda$  is 1.89. The inner wall of the duct is lined.

We started with an initial feasible solution of  $Z = \rho c$ , that is, with a lining having the characteristic impedance of air. The path followed during the perturbations of the impedance  $Z$  is shown in Figure 5. There, we have plotted the real and imaginary parts of  $Z$ . The heavy solid line traces the path taken by the impedance. The numbers beside the path points represent the fraction of power absorbed by the lining, that is,  $E_a/E_s$ . The  $\rho c$ -lining absorbs 57.6% of the energy. The final lining absorbs 92.4%. This is a 7.5 dB reduction in radiation from the  $\rho c$ -lining. Another calculation showed that it was an 11.2 dB reduction from the hard-wall case.

The calculation was repeated by starting with the lining that is found to be optimal by Rice for this case. We found that this lining absorbs 87.5% of the energy radiated by the piston. The numerical process moved the lining impedance from Rice's optimum to the same position as before. There is a 2 dB difference between the two linings. The close agreement between the numerical result and that of Rice is gratifying because it shows that the numerical method works properly.

Here are some more details about Figure 5. The heavy solid lines represent the perturbation paths taken by the numerical method. The grid of  $D/\lambda$  and  $L/D$  represent Rice's solutions for various ducts, and are put there to indicate the range of solutions that may be expected.

Table I shows details of the powers (or energies) absorbed as a fraction of radiated power. The dB-reductions are calculated relative to the  $\rho c$ -lining and the hard-wall cases. The calculated impedances are also given.

It was of interest to find how the absorption of energy was distributed along the lining. Figure 6 shows this distribution for the  $\rho c$ -lining, Rice's lining, and the optimal lining found by the present method. In the two latter cases, most of the energy is absorbed near the piston end of the duct.

In view of the uneven absorption of energy, the lining was split into two parts, in a length ratio 4/6, to attempt to increase the absorption at the piston end of the duct. Not much success was achieved in this regard, perhaps because of numerical difficulties that begin to appear as the ratio of absorbed to radiated energy approaches unity. More will be said of this later.

b) Bell-Mouth Duct

To assess the feasibility of using the method of optimization on a realistic duct shape, the bell-mouth duct of a 26-inch research compressor was studied. Its geometry is shown in Figure 7. The straight inner portion of the duct was lined as indicated. The blade sources were idealized as a piston actuator, and for this problem its frequency was 1500 Hz. It was assumed that 4 lobes were present in the circumferential acoustic field.

For a cylindrical duct with lobes, Kraft (Ref. 3) has presented an analysis for optimal linings similar to Rice's. We have used his analysis (even though in this example there is a large center body in the duct) to predict an initial feasible solution for this case.

In this particular example, which is of considerable complexity from a numerical standpoint, it was found to be more convenient to minimize the far field power  $E_f$ . The optimization process was carried out as far as practicable in terms of computer time. The best lining may not have been achieved, however.

Figure 8 illustrates the far field pressures at a distance of 15 feet from the mouth, plotted as a function of the angle from the axis of the duct. A study of this figure reveals that there are two pressure maxima: one at about  $35^\circ$  from the axis, the other toward the rear of the compressor (the latter maximum may not be physically significant, and no doubt arises because of the geometric idealizations performed on the original compressor). The optimization process attempts to reduce the total energy, rather than suppressing some particular pressure peaks. To this end, it has reduced the off-axis pressures at  $90^\circ$ , and the forward pressure peak. But it increased somewhat at the rear peak.

While the initial solution absorbed 91.8% of the source energy, the optimum absorbs 93.4%. The relative magnitudes of  $E_a$ ,  $E_s$  and  $E_f$  are shown in Table II. There, we show the results from two points of view. In the first table, the results are shown for a unit velocity at the piston. The far field energy is seen to be reduced by 1.7 dB from the initial solution. However, the energy balance ( $E_s - E_a = E_f$ ) is not very good. This is due to numerical difficulties, and more will be said of the problem. In the second table, the results are normalized to a constant source energy  $E_s$ . There, we observe that, in fact, there is an increase in  $E_f$ . In addition, the ratios of  $E_f$  for the two solutions is significantly different, with the same original data, but due to different normalization schemes. This observation leads us to conclude that there

may be a significant difficulty in comparing the results of an optimization process. Does one compare on the basis of velocity, pressure, or energy at the active source? The other conclusion is that numerical inaccuracies are certainly entering into the picture. After all,  $E_f$  is of the order of 1.6% to 1.8% of  $E_s$ , which is a rather small number in terms of total numerical accuracy. This comment brings us to the final point, that as the optimization process approaches a point where a significant amount of energy is absorbed (more than about  $0.9 E_s$ ), then the numerical accuracy becomes a critical factor. The desired accuracy can be achieved only at the expense of computer time, by increasing the geometric detail in the numerical scheme.

## VI. CONCLUSIONS

We believe that a method of lining optimization has been demonstrated. The results for a simple cylindrical duct were very encouraging. Significant difficulties of a numerical nature occur as the complexity of the problem increases. This is always true of any numerical procedure. Several points in particular may be noted. First, the precise mathematical description of an optimal lining may be difficult in view of the means of comparison -- should one normalize the results to the source velocity, pressure, or energy? In this connection, it appears desirable that the interaction between the blade rows and the duct acoustics be taken into account. Second, even with a simple geometry, as the optimum lining is approached, more accuracy is required in the calculations, since the far field energy becomes very small compared with the source energy, and its accurate calculation is essential to the numerical process. Such accuracy can be achieved at the expense of computer time. Finally, with an increase in frequency, more accuracy is also required, since the wavelengths are smaller.

In this report, we have assumed as a criterion for optimization that the absorbed energy should be maximized (or, what is the same thing, that the far field radiated energy should be minimized). As a result, we encountered in the bell-mouth duct a case where the far field pressure was reduced in one polar direction, while it was increased in another, although the far field energy was still minimized. This increased pressure may cause more annoyance than the original configuration. Thus, the proper selection of an optimization criterion is of extreme importance. In the last analysis, it would be desirable to use as a criterion that the annoyance factor during a specified maneuver be minimized. While this criterion may not be immediately feasible, it should be a goal to work towards.

## VII. REFERENCES

1. Tyler, J.M. and Sofrin, T.G., "Axial Flow Compressor Noise Studies," SAE Transactions, Vol. 70, 1962, pp. 309-332.
2. Rice, E.J., "Attenuation of Sound in Soft Walled Circular Ducts," NASA TM-X-52442, May 1968.
3. Kraft, R.E., "Sound Attenuation in a Lined Circular Duct in the Presence of Spinning Modes," General Electric TM 68-662, September 1968.
4. Liu, H.K. and Martenson, A.J., "Propagation of the Discrete Frequency Noise from Fans or Compressors in Axisymmetrical Ducts of Arbitrary Shape," To appear in the Journal of the Acoustical Society of America.
5. Evans, G.G., "General Purpose Parameter Optimization Sub-routines for the GE 625/635 Computer," General Electric TIS Report No. 67-C-156, April 1967.



Table I

## ENERGY ABSORPTION IN A CYLINDRICAL DUCT

<u>Lining</u>	<u>% Energy Absorbed</u>	<u>% Energy Radiated</u>	<u>dB Energy Reduction re <math>\rho c</math> Lining</u>	<u>dB Energy Reduction re Hard Walls</u>	<u>Re Z <math>\rho c</math></u>	<u>Im Z <math>\rho c</math></u>
Hard Wall	0	100	-3.8	0	-	-
$\rho c$	57.6	42.4	0	3.7	1	0
Rice's Optimum	87.5	12.5	5.3	9.0	1.17	-1.6
Single Lining	92.4	7.6	7.5	11.2	.82	-2.01
Split Lining (4/6)	93.6	6.4	8.2	11.9	.84 .775	-1.98 -2.04

Table II  
SUMMARY OF ENERGY CALCULATIONS

Normalized Velocity

Lining	$E_s$	$E_a$	$E_f$
Initial (Kraft)	1869	1717	30.5
Optimal	1125	1051	20.5

Normalized Source Energy

Lining	$E_s$	$E_a$	$E_f$
Initial (Kraft)	1000	918	16.32
Optimal	1000	934	18.2

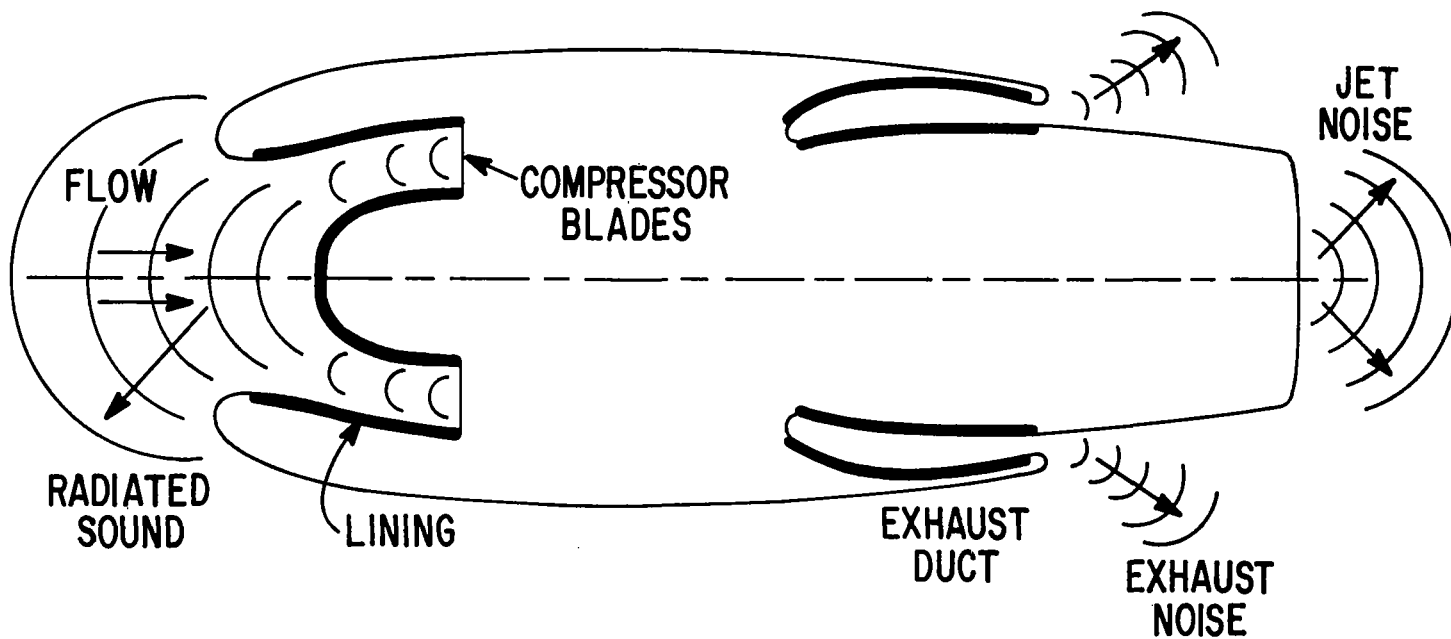


Fig. 1. Schematic of a Jet Engine.

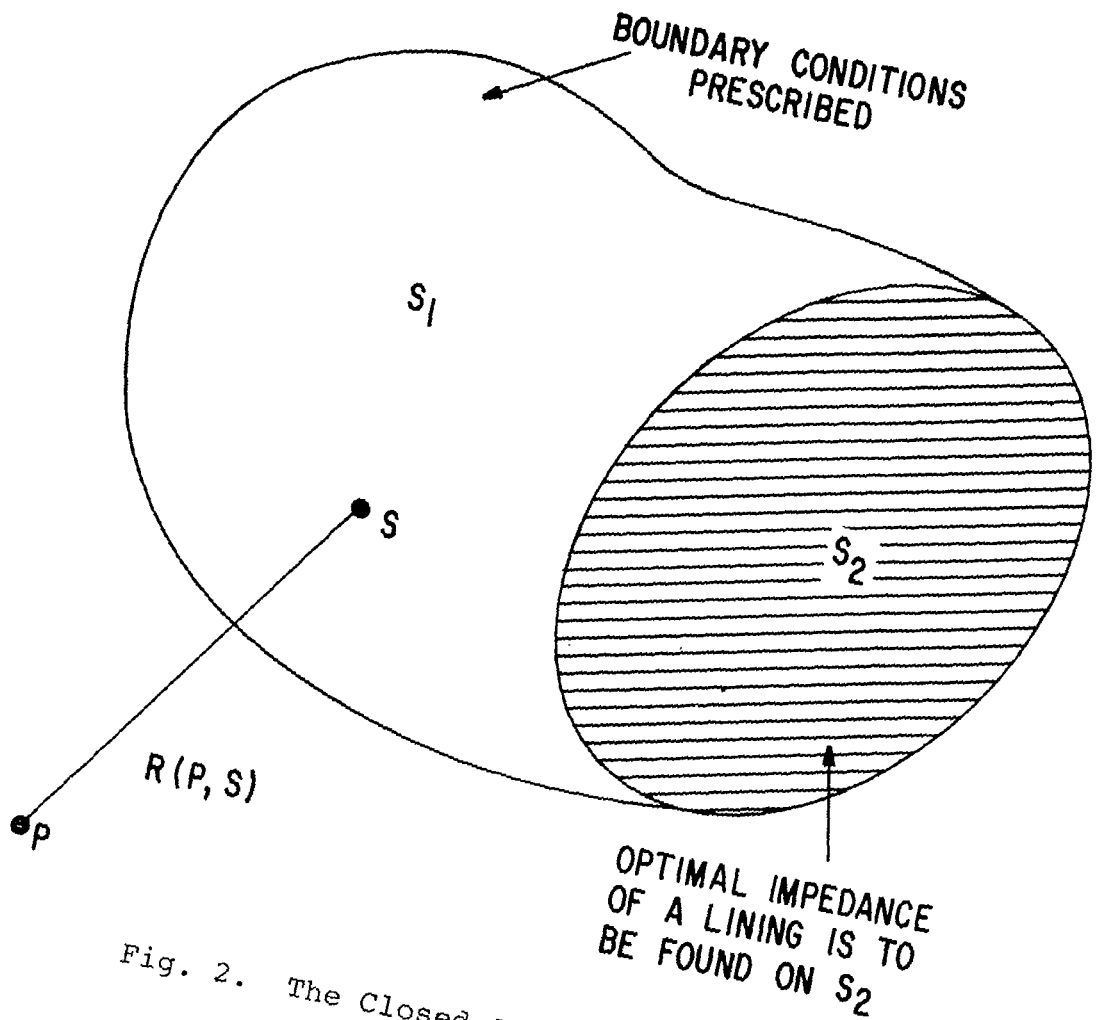


Fig. 2. The Closed Surface  $S_1 + S_2$ .

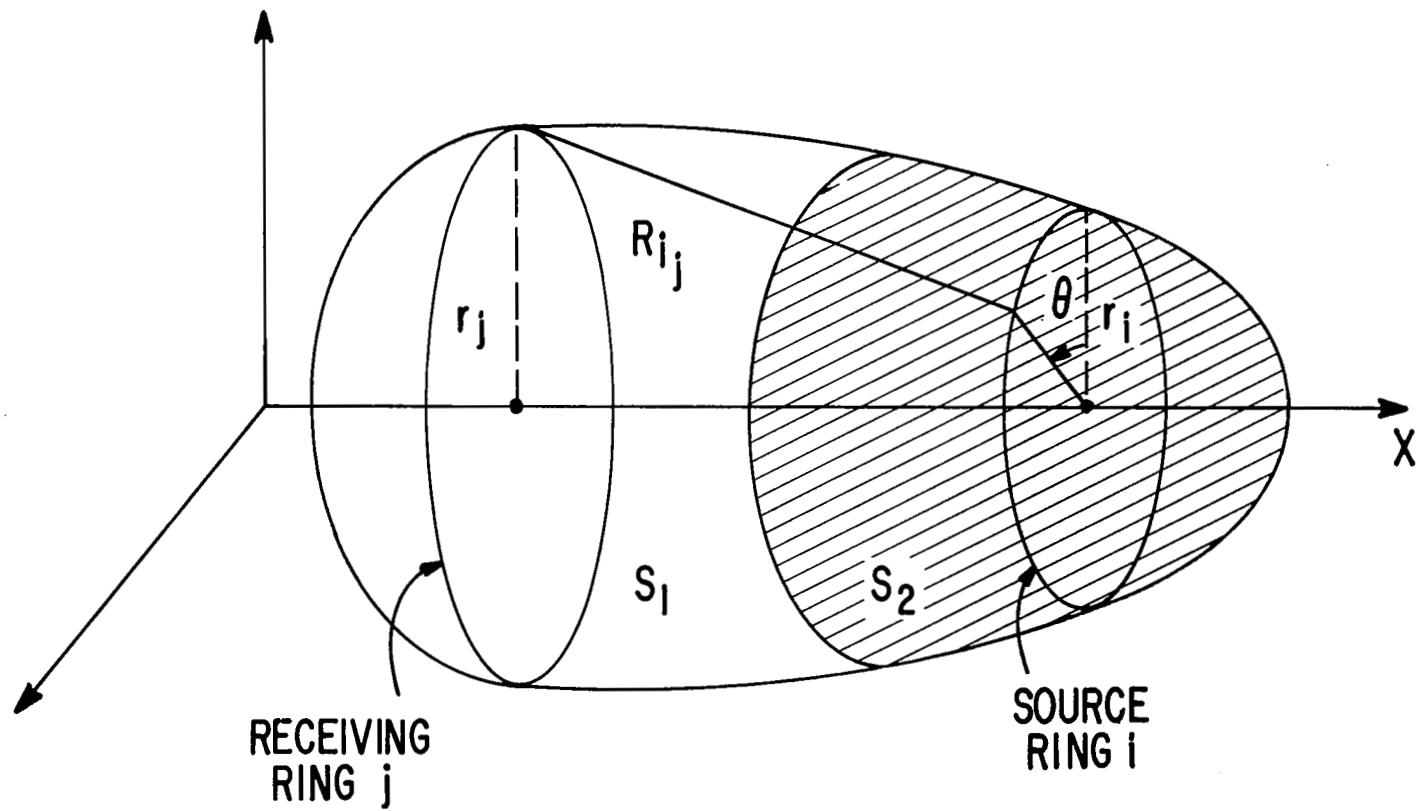


Fig. 3. Axially Symmetric Body in a Stationary Medium.

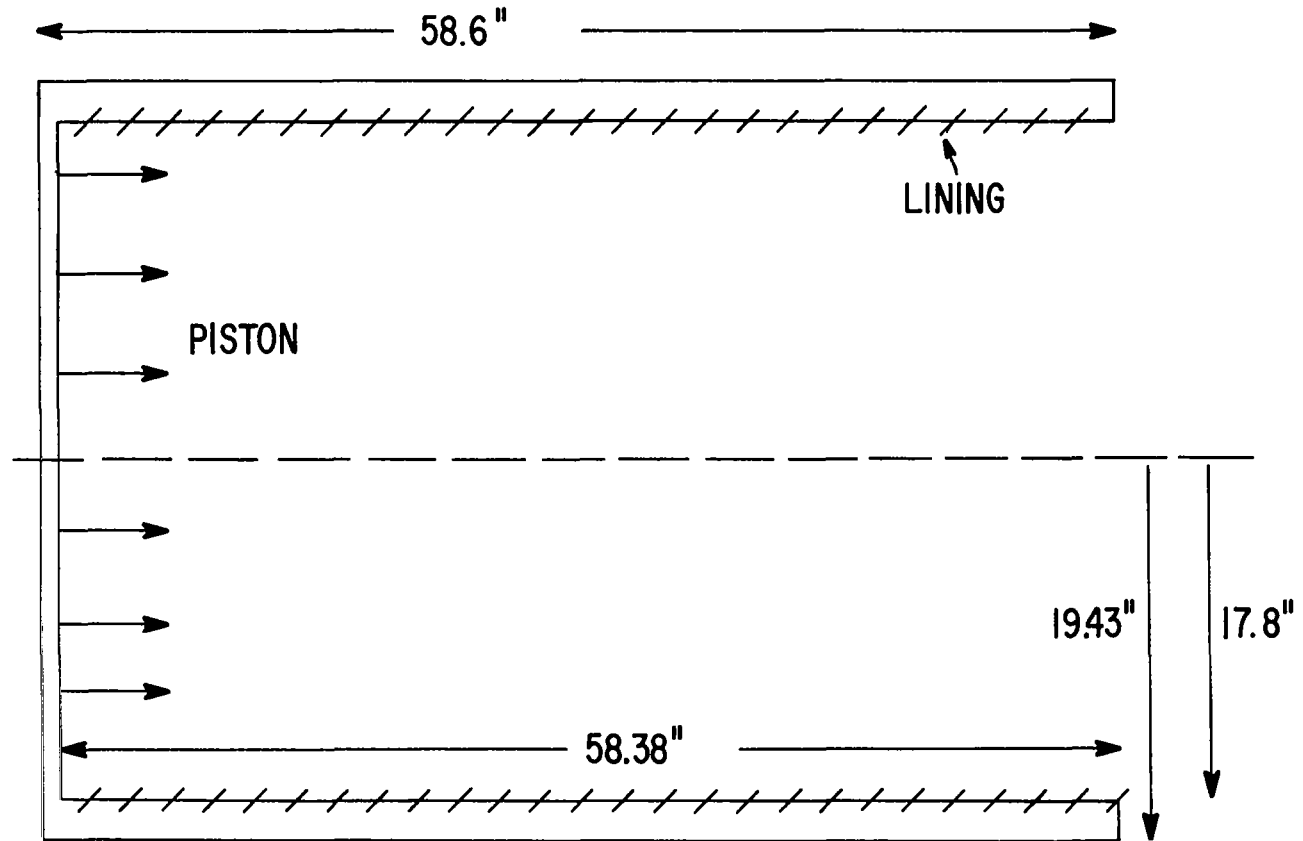


Fig. 4. Cylindrical Duct Geometry.

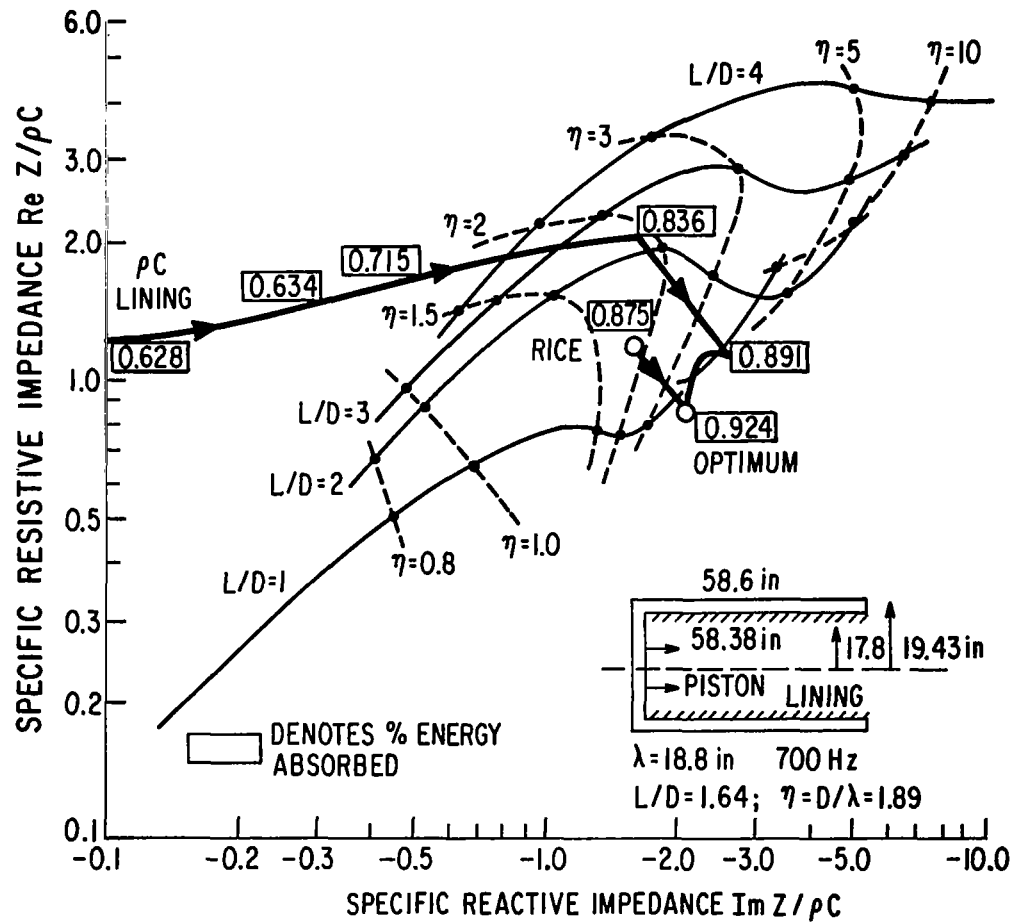


Fig. 5. OPTIMIZATION PATHS IN THE IMPEDANCE PLANE.

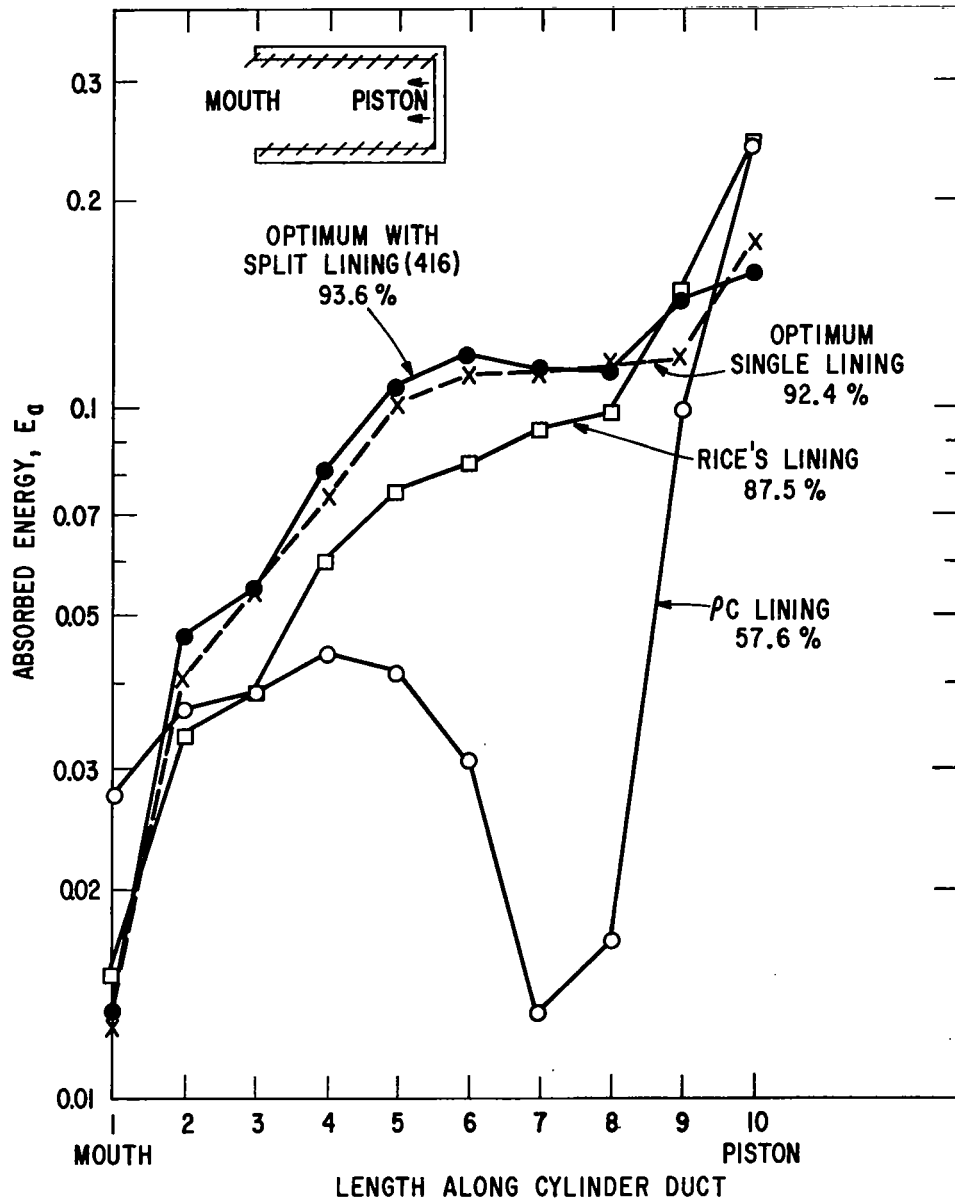


Fig. 6. Distribution of Absorbed Energy.



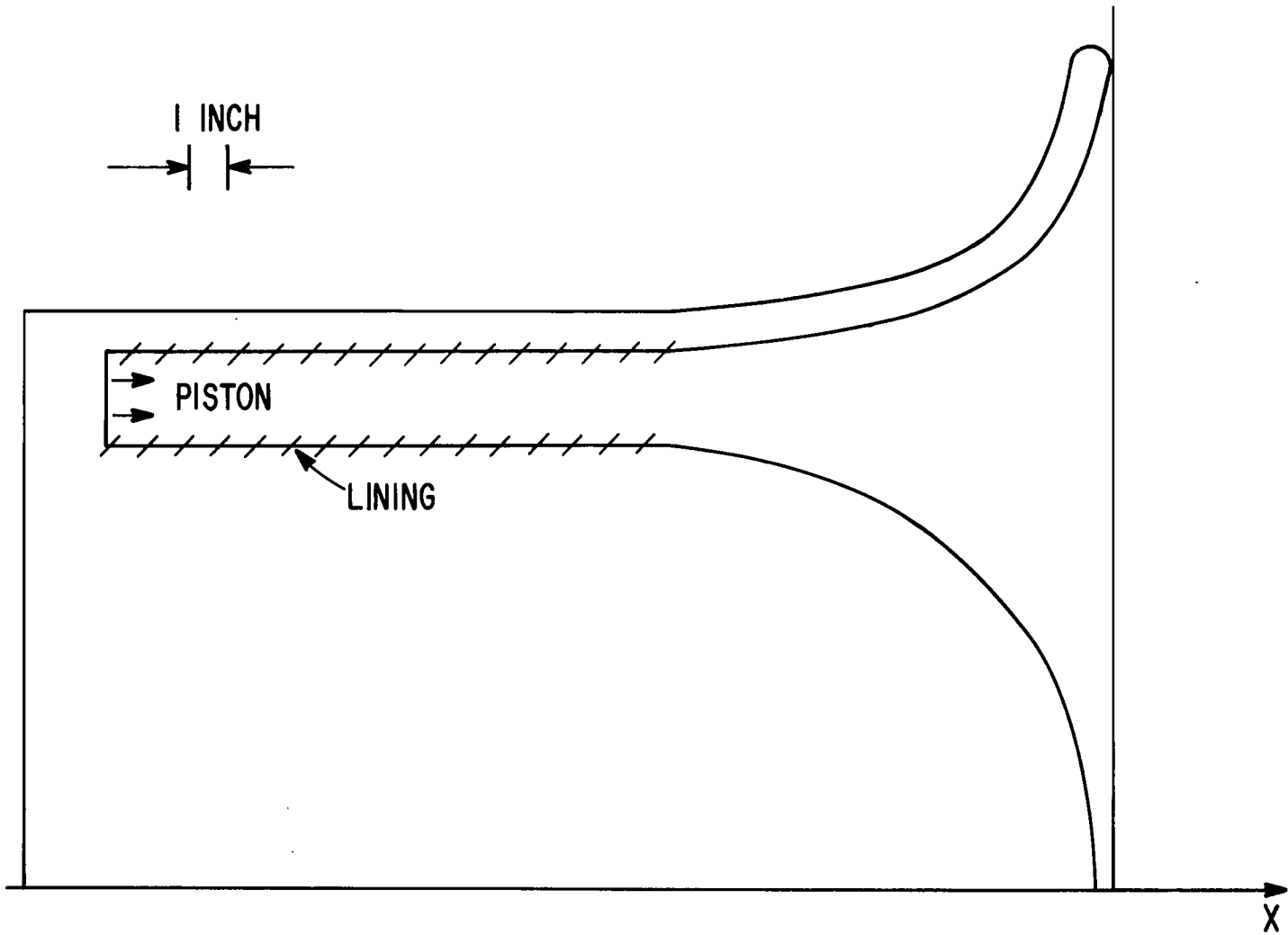


Fig. 7. Geometry of Bell-Mouth Duct.

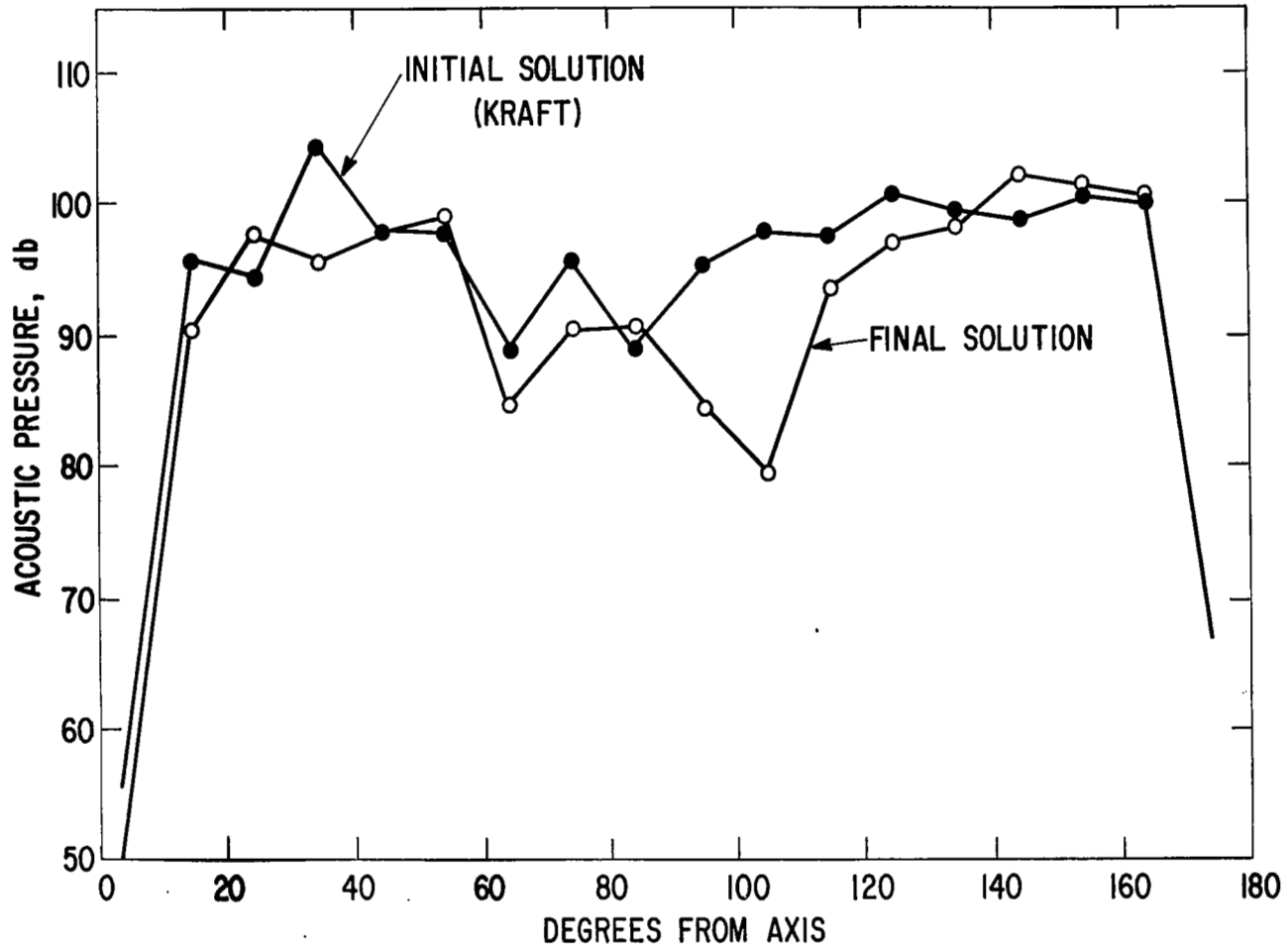


Fig. 8. Far Field Pressures at 15 Feet from the Duct Mouth.